

Back-angle anomalies in alpha scattering: Inelastic scattering from the calcium isotopes*

W. Trombik, K. A. Eberhard,[†] and J. S. Eck[‡]

Sektion Physik, Universität München, D-8046 Garching, Germany

(Received 26 August 1974)

Cross sections for elastic and inelastic α scattering on $^{40,42,44,48}\text{Ca}$ have been measured to several excited states. The bombarding energy (lab) is 24 MeV for $\alpha + ^{40,42,44}\text{Ca}$ and is 24 and 29 MeV for $\alpha + ^{48}\text{Ca}$. Particular emphasis is given to the back-angle data. In addition to the anomaly of $\alpha + ^{40}\text{Ca}$ elastic scattering at backward angles previously reported by many workers anomalous features are also observed in inelastic scattering. It is found that the backward anomaly of the $\alpha + ^{40}\text{Ca}$ inelastic cross sections is strongest for the 0^+ states and gradually decreases with increasing spins of the final states ($1^-, 3^-, 5^-$). The only exception is the scattering to the 2^+ state at 3.90 MeV, for which the cross sections exhibit a regular decrease toward backward angles. The inelastic cross sections for the $^{42,44,48}\text{Ca}$ isotopes are generally smaller at backward angles as compared to those for ^{40}Ca . In general, the observed anomalies for inelastic scattering at back angles are in close analogy to those known for elastic scattering. An interpretation of the data and of the anomalies in terms of coupled channels is given. Both a standard optical potential and one with an angular-momentum-dependent absorption have been used in the calculations. It is found that the large differences in the cross sections at backward angles, depending on the isotope and on the spin of the residual state, can be reproduced by coupled-channel calculations when an angular-momentum-dependent absorption in the optical potential is assumed.

$$\left[\begin{array}{l} \text{NUCLEAR REACTIONS } ^{40,42,44,48}\text{Ca}(\alpha, \alpha_0), ^{40,42,44,48}\text{Ca}(\alpha, \alpha'), E=24-29 \text{ MeV}; \\ \text{measured } \sigma(E, \theta); \text{ deduced coupled-channel parameters. Enriched targets; } \theta \\ = 12.5-177.5^\circ, \Delta\theta=2.5^\circ; \text{ calculated } \sigma(\theta). \end{array} \right]$$

I. INTRODUCTION

For many years the existing data on scattering of α particles from nuclei could be satisfactorily and easily parametrized by the concept of strong absorption. Models used for these calculations are the "strong absorption" models as, e.g., the Blair¹ and the Frahn-Venter model.² In the nuclear optical model the effect of strong absorption is taken into account by a complex potential with a rather deep imaginary potential well. The early success of these models to describe α scattering seems to be primarily due to the fact that those scattering data were measured and fitted at forward angles only.

During the last 10 years, however, an increasing number of α -scattering angular distributions were measured, which extended to the back-angle hemisphere. For a great number of them a so-called "anomalous" scattering behavior was observed at backward angles: In contrast to the "normal" angular distributions which exhibit a diffractionlike pattern and an over-all decrease of the cross section with scattering angle—as also predicted by the optical model—angular distributions for the α scattering from some target nuclei

were obtained where the cross sections increased strongly toward backward angles. This anomalous large angle α scattering ("ALAS") has been of increasing interest in recent years and has been the subject of symposiums at Marburg³ and at Cracow.⁴ Similar effects have also been observed in excitation functions and angular distributions for heavy ion scattering,^{5,6} in particular for the scattering of ^{16}O on ^{16}O (Ref. 5). For the $^3\text{He} + ^{40}\text{Ca}$ elastic scattering and possibly for $^3\text{He} + ^{39}\text{K}$ only a slight increase of the cross section toward backward angles is observed, although it is much weaker than for α scattering,^{7,8} and no enhancement has been found in any other ^3He scattering data.

Whereas a rather comprehensive set of experimental back-angle data exists for elastic α scattering from various target nuclei, only a few appropriate data for inelastic scattering are available. A survey on these inelastic data is provided in Table I. As indicated in Table I, a back-angle enhancement of the cross sections is observed for some target nuclei between ^{12}C and ^{40}Ca ; a behavior which is similar to that for elastic scattering. Most of these inelastic measurements, however, have been performed at energies where strong compound contributions are likely to be

TABLE I. Survey of experimental data for inelastic α scattering at backward angles. In column 2 the lowest and highest bombarding energies (lab) are listed at which data were taken. A "yes" in column 3 indicates a back-angle anomaly, a "no" means that no particular back-angle enhancement is observed, a "(yes)" stands for a behavior in between.

Target	Bombarding energies (lowest, highest) [MeV(lab)]	Back-angle enhancement	References
^{12}C	6; 35.5	yes	9-13
^{16}O	18; 22.5	(yes)	10, 14
^{18}O	21.4	no	15
^{20}Ne	16.8; 18.0	(yes)	16, 17, 18
^{23}Na	18.0	yes	18
^{24}Mg	10.8; 80.0	(yes)	19-27
^{27}Al	18.7	yes	28
^{28}Si	16.2; 28.0	yes	14, 29, 30, 31
^{31}P	18.2; 26.5	yes	18, 31, 32
^{32}S	18; 26.5	yes	10, 31
^{40}Ar	18	no	17, 18
^{40}Ca	24; 29	yes	33, Present work
^{42}Ca	24	(yes)	Present work
^{44}Ca	24	(yes)	Present work
^{48}Ca	24; 29	(yes)	Present work
^{56}Fe	22.2	no	34
^{58}Fe	21.0	no	35
^{58}Ni	13; 29	no	35-40
^{60}Ni	18; 27	no	38
^{62}Ni	18; 27	no	35, 38
^{64}Ni	18; 27	no	35, 37, 38, 39
^{63}Cu	19.5	no	37
^{64}Zn	21; 22.2	no	34, 35
^{68}Zn	19.5; 22.2	no	34, 37
^{68}Zn	22.2; 23.3	no	34, 39

present. Thus, any backward increase of the cross section could be caused by the compound part of the reaction. For target nuclei in Table I heavier than calcium and at incident energies of 20 MeV or more, where compound contributions should be negligible, no back-angle increase is observed. This is in agreement with the results for elastic scattering. For the mass-energy region where the strongest back-angle anomalies for elastic scattering were obtained, i.e., around $A=40$ and $E_\alpha=20$ through 30 MeV, no comparable data exist for inelastic α scattering. The only observation of a backward enhancement of inelastic α scattering in this region was reported by Schmeing and Santo³³ who measured $\alpha + ^{40}\text{Ca}$ scattering at 29 MeV. It is the aim of this paper to present angular distributions for the inelastic $\alpha + ^{40,42,44,48}\text{Ca}$ scattering for a detailed comparison with the elastic data. In particular, the question is investigated whether the large differences of two orders of

magnitude between $\alpha + ^{40}\text{Ca}$ and $\alpha + ^{44}\text{Ca}$ elastic scattering cross sections at backward angles also exist in inelastic scattering.

Theoretical investigations of the back-angle anomalies have been confined almost entirely to elastic scattering. The complete understanding of the origin of the anomalies seems to remain to be an open question at present, although several approaches have been suggested, which relate the observed anomalies either to structure effects (mainly "exchange") or to reaction mechanism effects (angular-momentum-dependent absorption). For a discussion of this interesting phenomenon we refer to the proceedings of the recent conferences on this subject at Marburg³ and at Cracow⁴ and to the literature cited therein. The earliest and apparently most successful of these approaches has been the extended optical model with an angular-momentum-dependent absorption, as suggested by Robson and first developed and applied to experimental data by the Florida State group.^{6,41,42} An outline of this model is given in Sec. IV.

We would like to point out that the modified optical model with angular momentum dependent absorption is, at present, the only explanation of back-angle anomalies which has been extended to allow the calculation of *inelastic* cross sections. An analysis of our data in terms of this model is given in Sec. IV. The experiment is described in Sec. II and the experimental results are summarized in Sec. III.

II. EXPERIMENT

Angular distributions for elastic and inelastic α scattering on $^{40,42,44,48}\text{Ca}$ were measured at 24 MeV bombarding energy (lab) for the angular range 12.5 through 177.5° (lab) in 2.5° steps. For $\alpha + ^{48}\text{Ca}$ scattering, data were also taken at 29 MeV. An intense α -particle beam (~500 nA) from the Munich MP tandem was focused onto the target in the center of the 80 cm scattering chamber.⁴³ The scattered particles were detected in an array of up to 10 Si surface barrier detectors. The pulses from the detectors were recorded in the standard way. Each spectrum was analyzed with a separate analog-to-digital converter (ADC) interfaced to the Munich PDP-8/PDP-10 computer system. Dead time corrections were made by measuring the charge accumulated for each ADC only during the time which that ADC was alive. The detectors used were made by Kemmer and co-workers in our laboratory. They are silicon surface barrier detectors and are rectangular in size (22 mm×9 mm); these detectors combine the advantage of a large solid angle with a good angular resolution,

which is of particular importance for measurements of small cross sections such as at backward angles.

Thin targets for the calcium isotopes (~ 50 to $100 \mu\text{g}/\text{cm}^2$) were obtained by evaporating the calcium onto thin carbon foils ($\sim 30 \mu\text{g}/\text{cm}^2$). They were then transferred to the scattering chamber by an air-lock system to avoid oxidation. A typical particle spectrum is shown in Fig. 1 for the $\alpha + {}^{42}\text{Ca}$ scattering at 24 MeV at 170° (lab). The ${}^{42}\text{Ca}$ target contained about 5% of ${}^{40}\text{Ca}$ and the ${}^{40}\text{Ca}$ lines are clearly seen in the spectrum. As a by-product, this spectrum may serve to demonstrate the strong enhancement of the elastic and inelastic $\alpha + {}^{40}\text{Ca}$ cross sections over those for $\alpha + {}^{42}\text{Ca}$ at backward angles.

The relative solid angle of each detector was determined by measuring the α -particle cross section from a thin gold foil at 12 MeV bombarding energy. At this energy the forward-angle scattering is pure Rutherford scattering. The absolute normalization of the various $\alpha + \text{Ca}$ cross sections was obtained by comparing the forward-angle scattering at $E_\alpha(\text{lab}) = 12 \text{ MeV}$ to calculations of Rutherford scattering. The absolute normalization is accurate to $\pm 8\%$.

III. EXPERIMENTAL RESULTS

In Fig. 2 angular distributions for the elastic and inelastic α scattering from ${}^{40}\text{Ca}$ and ${}^{44}\text{Ca}$ at $E_\alpha(\text{lab}) = 24 \text{ MeV}$ are compared. The increase of the cross sections toward backward angles is stronger for the $\alpha + {}^{40}\text{Ca}$ and is less pronounced in case of $\alpha + {}^{44}\text{Ca}$. For $\alpha + {}^{40}\text{Ca}$ it is clearly seen from Fig. 2 that the enhancement of the cross section is closely related to the spins of the corresponding excited states: The backward enhance-

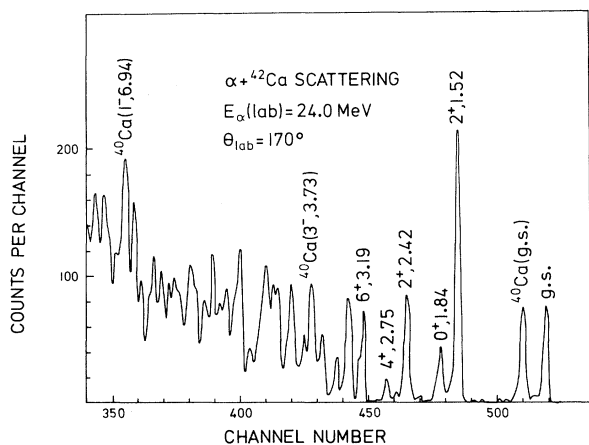


FIG. 1. Particle spectrum for $\alpha + {}^{42}\text{Ca}$ scattering at 170° (lab) and at $E_\alpha(\text{lab}) = 24 \text{ MeV}$.

ment of the cross sections is strongest for the 0^+ states and gradually decreases with the spin of these levels. A similar behavior had been observed earlier at $E_\alpha(\text{lab}) = 29 \text{ MeV}$ ^{33,34} with the only exception of the 2^+ (3.90 MeV) state which shows a pronounced decrease of the cross section with angle. The scattering to this state which is separated by less than 150 keV from the strongly excited 3^- (3.73 MeV) state could not satisfactorily be resolved in this work; in agreement with Ref. 33, however, an estimate of this state yielded a strongly decreasing cross section toward backward angles. An explanation for the exceptional behavior of the scattering to this 2^+ state as compared

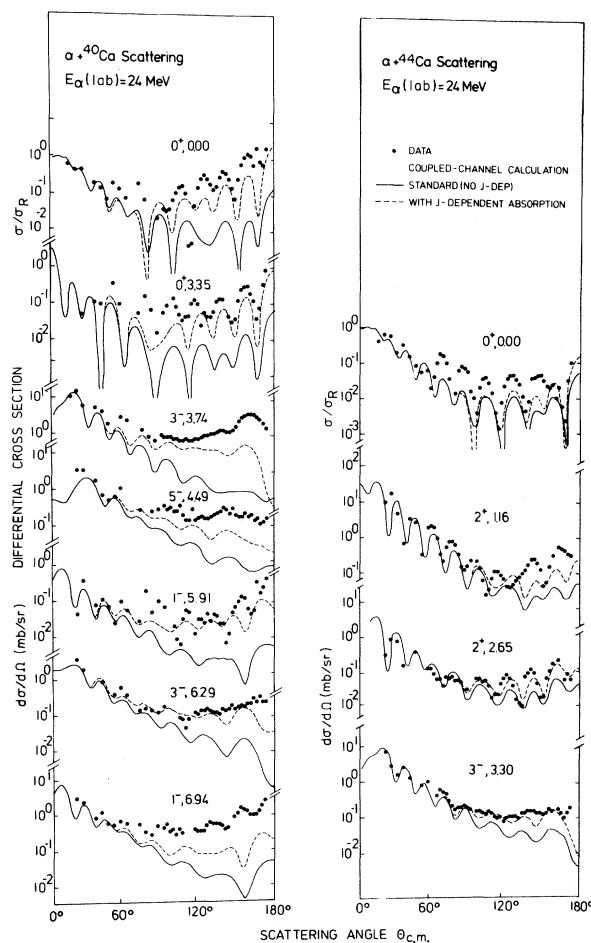


FIG. 2. Experimental and calculated angular distributions for the elastic and inelastic scattering of α particles from ${}^{40}\text{Ca}$ (left-hand side) and from ${}^{44}\text{Ca}$ (right-hand side) at a bombarding energy of 24 MeV . The solid curves represent coupled-channel calculations using a standard four-parameter optical potential, the dashed ones are calculations for a potential with angular-momentum-dependent absorption. The coupling parameters are listed in Table II, those for the optical potential are given in Table III.

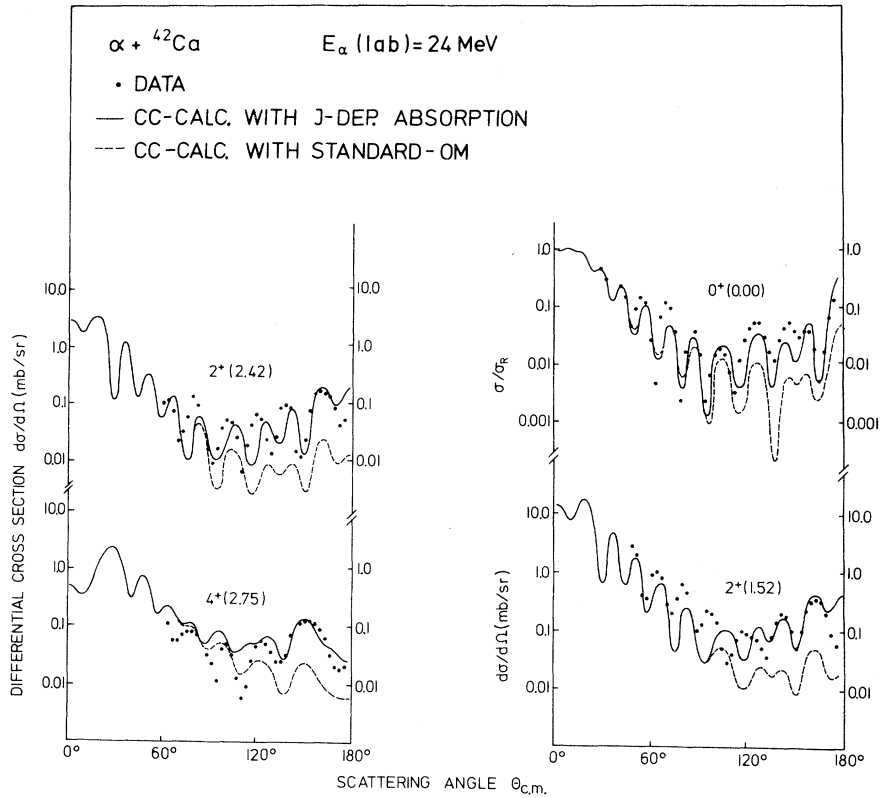


FIG. 3. Same as in Fig. 2, but for $\alpha + {}^{42}\text{Ca}$ scattering.

to the others has not yet been found. For further details we refer to Ref. 44.

A clear distinction has been made for the scattering of $\alpha + {}^{40}\text{Ca}$ as being "anomalous" and for $\alpha + {}^{44}\text{Ca}$ as being "normal" on the basis of the elastic scattering data. The inclusion of the inelastic data, as presented in Fig. 2, supports this distinction although it becomes less rigorous and a certain increase of the inelastic cross section for the two 2^+ states at 1.16 and 2.65 MeV is seen.

In Fig. 3 angular distributions for $\alpha + {}^{42}\text{Ca}$ scattering are depicted. Again an increase of the inelastic cross sections (as well as the elastic ones) toward backward angles is observed. It is interesting to note that the cross sections at backangles are very similar for the 2^+ (1.52 MeV) state in ${}^{42}\text{Ca}$ and the 2^+ (1.16 MeV) state in ${}^{44}\text{Ca}$ on the one hand, and for the 2^+ (2.42 MeV) state in ${}^{42}\text{Ca}$ and the 2^+ (2.65 MeV) state in ${}^{44}\text{Ca}$ on the other hand—both in shape and in absolute magnitude. The scattering to the 4^+ (2.75 MeV) state in ${}^{42}\text{Ca}$ also shows an over-all increasing cross section toward backward angles which is comparable to the behavior of the 2^+ states. Consequently, in case of $\alpha + {}^{42}\text{Ca}$ the decreasing enhancement of the back-angle cross sections with spin, as found for $\alpha + {}^{40}\text{Ca}$, does not hold here—as far as the limited information of

only three excited states allows to make such a statement.

For the $\alpha + {}^{48}\text{Ca}$ scattering only the elastic scattering and the inelastic scattering to the first excited 2^+ (3.83 MeV) state could be measured with sufficient accuracy. Figure 4 summarizes the results obtained at $E_\alpha(\text{lab}) = 24$ and 29 MeV. The 0^+ (4.28 MeV) state, following the 2^+ (3.83 MeV) state in the level scheme, is very weakly excited, whereas the 3^- (4.51 MeV) state—which would be very interesting for a comparison with the other isotopes—is strongly excited; however, it could not be resolved from the state at 4.61 MeV, which is also strongly excited. The angular distribution for the scattering to the 2^+ (3.83 MeV) state again is rather similar to the corresponding ones for ${}^{42}\text{Ca}$ and ${}^{44}\text{Ca}$.

With regard to the anomalies observed for the elastic scattering one may summarize the experimental results for the inelastic scattering of α particles from the Ca isotopes on the basis of the data presented here in the following way: Only the scattering to the low-spin states in ${}^{40}\text{Ca}$, i.e., the 0^+ and 1^- states, exhibits an over-all increase of the cross section between 90 and 180° comparable to the strong enhancement as observed for the elastic $\alpha + {}^{40}\text{Ca}$ scattering. For the other states

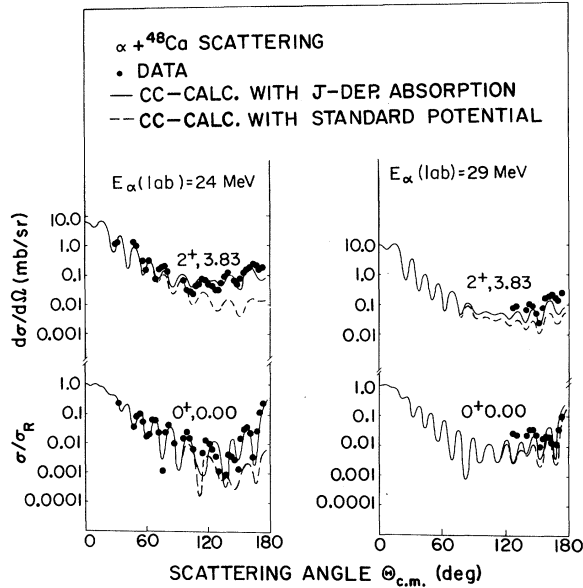


FIG. 4. Same as in Fig. 2, but for $\alpha + {}^{48}\text{Ca}$ scattering.

in ${}^{40}\text{Ca}$ there is still some increase toward backward angles; and even for the states in ${}^{42,44,48}\text{Ca}$ this effect is observed although it is much weaker there.

IV. ANALYSIS OF INELASTIC DATA

The inelastic cross sections as presented in the previous section are analyzed in this section in terms of coupled-channel calculations. The use of the coupled-channel approach rather than a distorted-wave Born-approximation approach is motivated by the fact that the 3^- states around 3.5 MeV excitation energy in the calcium isotopes are much more strongly excited in inelastic α scattering than any other state and thus should be included when inelastic cross sections are computed. Comparative calculations with and without coupling through the 3^- state clearly indicated the necessity of including the 3^- state in the calculations. In particular, a satisfactory agreement with the data could only be achieved in this way and could not be gained by coupling the state under consideration solely to the ground state. For the calculations presented here we have assumed a vibrational form factor with complex coupling; i.e., the imaginary as well as the real potential is deformable.

We would like to note at this point that one might not *a priori* expect strong collective excitations for the doubly magic nucleus ${}^{40}\text{Ca}$. In recent years, however, several authors have reported evidence for a collective nature of some of the low-lying states in ${}^{40}\text{Ca}$. These results are sup-

ported by the data presented here, although this point is beyond the scope of the present paper and is not discussed here. The main purpose of the present paper is an analysis of the back-angle data in an attempt to describe the observed anomalies.

For elastic scattering it has been shown that the orders-of-magnitude difference at back angles for, e.g., $\alpha + {}^{40}\text{Ca}$ and $\alpha + {}^{44}\text{Ca}$ scattering can be reproduced by assuming an angular-momentum-dependent absorption in the optical model potential.⁴² The imaginary potential W in the optical model parametrizes the absorption of the incoming waves into reaction and inelastic channels, and in the standard optical model is the same for all incoming partial waves. In case of heavy ion and α scattering, however, the incoming partial waves may bring into the reaction area larger orbital angular momenta than can be carried away by most of the reaction and/or inelastic channels. Consequently, the absorption for those high partial waves is less than it is for lower partial waves, so that the contributions from the higher partial waves remain in the elastic channel. The elastic cross section is then dominated by these high partial waves, i.e., the strength of the backward enhancement depends critically on the angular momentum mismatch between the elastic and the nonelastic channels.⁴² To account for this effect the absorption potential W in optical model calculations has been made angular-momentum-dependent by assuming the Woods-Saxon form derived and discussed by Chatwin, Eck, Robson, and Richter⁶:

$$W(r, J) = W(r) \{1 + \exp[(J - J_c)/\Delta J]\}^{-1}, \quad (1)$$

where $\vec{J} = \vec{L} + \vec{I}_1 + \vec{I}_2$ is the angular momentum in the nonelastic channels with L being the orbital angular momentum and I_1 and I_2 being the spins of the particles in that channel. The quantity J_c is an average characteristic cutoff in angular momentum for the nonelastic channels and ΔJ_c is its diffuseness.^{6,42} We would like to point out that in the case of elastic scattering of a spin-zero target nucleus $J = L$, and the absorptive potential reduces to an L -dependent one. This simple form has been used in analyses for a large number of elastic scattering data and has given considerable support to the model.^{6,41,42,44,45,46}

An extension of this model for *inelastic* scattering has recently been developed by Cramer *et al.*⁴⁴ in terms of coupled channels and has been applied successfully to $\alpha + {}^{40}\text{Ca}$ inelastic scattering at 29 MeV. The computer code JUPITOR by Tamura⁴⁷ (Karlsruhe version⁴⁸) was changed to have an absorption of the form of Eq. (1).

In the following, coupled-channel calculations with and without angular-momentum-dependent (J -dependent) absorption are compared. To be as

TABLE II. Coupling strength parameters as used in the coupled-channel calculations with the modified code JUPITOR (Refs. 46 and 47), where β_3 corresponds to the 3⁻ state and β_I to the third state coupled.

Reaction	Coupling scheme	β_I	β_3
$\alpha + {}^{40}\text{Ca}$	$0^+(\text{g.s.})-0^+(3.35)-3^-(3.74)$	0.035	0.25
	$0^+(\text{g.s.})-2^+(3.90)-3^-(3.74)$	0.12	0.25
	$0^+(\text{g.s.})-5^-(4.49)-3^-(3.74)$	0.15	0.25
	$0^+(\text{g.s.})-1^-(5.91)-3^-(3.74)$	0.05	0.25
	$0^+(\text{g.s.})-3^-(6.29)-3^-(3.74)$	0.15	0.25
	$0^+(\text{g.s.})-1^-(6.94)-3^-(3.74)$	0.18	0.25
	$0^+(\text{g.s.})-0^+(7.30)-3^-(3.74)$	0.10	0.25
$\alpha + {}^{42}\text{Ca}$	$0^+(\text{g.s.})-2^+(1.52)-3^-(3.44)$	0.19	0.30
	$0^+(\text{g.s.})-2^+(2.42)-3^-(3.44)$	0.092	0.30
	$0^+(\text{g.s.})-4^+(2.75)-3^-(3.44)$	0.107	0.30
$\alpha + {}^{44}\text{Ca}$	$0^+(\text{g.s.})-2^+(1.16)-3^-(3.30)$	0.25	0.20
	$0^+(\text{g.s.})-2^+(2.65)-3^-(3.30)$	0.10	0.20
$\alpha + {}^{48}\text{Ca}$	$0^+(\text{g.s.})-2^+(3.83)$	0.13	

consistent as possible concerning the optical potential parameters we have used the same potential for all nuclei of interest here, and have used the parameter set of Gaul *et al.*⁴⁹ found from elastic scattering analyses for a large number of target nuclei in this mass region. These parameter values are listed in Table II. The imaginary potential depth of originally 26.6 MeV (Ref. 49) was reduced to 23.6 MeV to compensate for the explicit coupling to some excited states in the coupled-channel calculations. Following Gaul *et al.*⁴⁹ we have used a slightly different potential for $\alpha + {}^{48}\text{Ca}$ scattering (see Table II); here the absorption was reduced from 29 to 26 MeV.

The parameters J_c and ΔJ in Eq. (1), describing the angular momentum dependence of the absorption in the optical potential, have been obtained in the following way: Following earlier investigations of elastic α scattering on calcium using the angular-momentum-dependent absorption model^{42,50} we have maintained a value of $\Delta J = 2.5$ throughout the calculations. It has been shown in Ref. 42 that other values for ΔJ , ranging from about $\Delta J = 0.5$ to 5.0, can be consistently compensated by a small uniform change in the J_c values. The only parameter which was varied in the coupled-channel calculations is the angular momentum cutoff parameter J_c . The values obtained are summarized in Table III. It is gratifying to note that these values are very close to those found in earlier investigations of elastic scattering.^{42,50} It is seen from Table III that the value for the angular momentum cutoff parameter J_c is smallest for ${}^{40}\text{Ca}$ ($J_c = 11.4$) and largest for ${}^{44}\text{Ca}$ ($J_c = 15$) at a bombarding energy of 24 MeV. Since the values of J_c represent the average maximum angular momentum which

TABLE III. Parameter values for the optical potential used in the coupled-channel calculations (coupling strength parameters see Table II); $R = r_0 A_T^{1/3}$.

Target	E_α (MeV)	V (MeV)	W (MeV)	r_0 (fm)	a (fm)	J	J_c
${}^{40}\text{Ca}$	24.0	183.7	23.6	1.392	0.564	2.5	11.4
${}^{42}\text{Ca}$	24.0	183.7	23.6	1.392	0.564	2.5	13.0
${}^{44}\text{Ca}$	24.0	183.7	23.6	1.392	0.564	2.5	15.0
${}^{48}\text{Ca}^a$	24.0	183.7	26.0	1.40	0.564	2.5	12.9
${}^{48}\text{Ca}^a$	29.0	183.7	26.0	1.40	0.564	2.5	17.5

^a Following Ref. 49 a slightly different form factor was used for the imaginary potential by changing the diffuse-ness parameter to $a_i = 0.5116$ fm.

can be carried away in nonelastic channels this difference reflects the fact that in case of $\alpha + {}^{40}\text{Ca}$ the absorption of high partial waves around $l \approx 11$ is much less than it is for $\alpha + {}^{44}\text{Ca}$ scattering, where these partial waves are still strongly absorbed. This difference in the absorption, i.e., in the J_c values, for different isotopes and nuclei has been studied in detail in Refs. 42, 50, and 51. It has been related to different reaction Q values for these nuclei, which through different level densities in the corresponding compound and residual nuclei result in different maximum angular momenta which can be carried in those channels. A reasonable dependence of the J_c values on the mass and the structure of the target nuclei as well as on the energy is a major test for the angular-momentum-dependent absorption model. This question has been studied in detail for heavy ion scattering^{6,46} and for α scattering^{41,42,50,51} and has given considerable support to the model.

To study the effect of an angular-momentum-dependent absorption on the inelastic cross sections, we have also calculated cross sections with a standard optical potential for comparison. The coupling schemes and strengths used in the calculations are summarized in Table II; the potential parameters are given in Table III. The results are shown in Fig. 2 along with the experimental data. The calculated cross sections for the 0^+ (g.s.) and the $3^-(3.74)$ MeV state depend slightly on the choice of the additional state to which they are coupled. The calculated cross sections for the 0^+ (g.s.) and $3^-(3.73)$ MeV state presented in Fig. 2 were obtained by coupling only these two states together.

The results for $\alpha + {}^{44}\text{Ca}$ scattering (see Fig. 2) were obtained also by a vibrational coupling of the 0^+ (g.s.)- 1^- - $3^-(3.30)$ MeV states. In contrast to the results for $\alpha + {}^{40}\text{Ca}$, the elastic and inelastic $\alpha + {}^{44}\text{Ca}$ scattering does not exhibit a strong backward enhancement of the cross sections and hence is in an-order-of-magnitude better agreement with

standard optical model and “coupled-channel” calculations than in the case of $\alpha + {}^{40}\text{Ca}$. Whereas the cross sections at forward and at backward angles are approximately the same for $\alpha + {}^{40}\text{Ca}$ (see Fig. 2), they fall off for $\alpha + {}^{44}\text{Ca}$ by at least one order of magnitude from forward to backward angles. It is interesting to note that a relatively weak angular momentum dependence of the absorption for $\alpha + {}^{44}\text{Ca}$ ($\Delta J = 2.5$, $J_c = 15.0$) has but little effect on the elastic cross sections; the inelastic cross sections, however, are strongly influenced. This leads to considerably better agreement with the experimental data.

A clear improvement in the agreement between data and calculations is also seen for the $\alpha + {}^{42}\text{Ca}$ scattering in Fig. 3 and for $\alpha + {}^{48}\text{Ca}$ scattering in Fig. 4, when an angular-momentum-dependent absorption is used for the potential instead of the standard one.

At the end of this section we would like to discuss the possibility of compound contributions in the data presented here. Compound contributions in elastic $\alpha + {}^{40}\text{Ca}$ scattering between $E_\alpha = 5$ and 18 MeV have been studied in great detail by Bisson, Eberhard, and Davis.⁴¹ On the basis of Ericson-type fluctuation analyses of the excitation functions, Hauser-Feshbach analyses of the angular distributions, and theoretical estimates from the Fermi-gas model, a consistent and rapid decrease of the compound contribution above $E_\alpha = 10$ MeV, where it is largest, to less than a few percent at $E_\alpha = 18$ MeV was found. An extrapolation to energies of $E_\alpha = 24$ and 29 MeV where our data were taken leads to negligible compound contributions. This result is confirmed by the work of Gaul *et al.*⁴⁹ who have measured excitation functions for $\alpha + {}^{40}\text{Ca}$ elastic scattering at several backward angles between $E_\alpha = 27$ and 28 MeV and have obtained smooth excitation functions without any indication of Ericson-type fluctuations. Compound contributions of a few percent would already result in pronounced Ericson-type fluctuations for a “one-channel-re-

action” such as elastic $\alpha + {}^{40}\text{Ca}$ scattering (see, e.g., Ericson and Mayer-Kuckuk⁵²).

V. CONCLUSIONS

As a main result of this paper back-angle anomalies for inelastic α scattering from the calcium isotopes are reported. A strong backward enhancement of the cross sections is observed for $\alpha + {}^{40}\text{Ca}$, whereas the cross sections for $\alpha + {}^{44}\text{Ca}$ are at least one order of magnitude smaller. Generally, the inelastic data are in close relation to the anomalies observed previously for elastic scattering. Coupled-channel calculations using potentials with angular-momentum-dependent (J -dependent) absorption reproduce the absolute magnitude of the back-angle cross sections, whereas calculations with standard potentials fail to do so by, partly, orders of magnitude. The $\alpha + {}^{40}\text{Ca}$ data show a decreasing enhancement of the cross sections at backward angles with increasing spin of the final state. This effect (with the exception^{33,44} of the 2^+ state at 3.90 MeV) is well accounted for by the coupled-channel calculations with J -dependent absorption. The concept of using an angular momentum dependent absorption in optical potentials is therefore interpreted as a useful procedure to parametrize the scattering results observed. It furthermore leads to a model—being the only one at present—which can reproduce the observed anomalies both for elastic *and* inelastic scattering.

ACKNOWLEDGMENTS

We would like to thank E. Mathiak, J. Schiele, J. Stettmeier, and Dr. H. H. Rossner for their help during various runs of the experiment as well as Dr. K. E. Rehm for his assistance with the scattering chamber. We are pleased to acknowledge Frau Weismann and Dr. J. Kemmer for fabrication of the solid state detectors, and Fräulein Frischke and Dr. H.-J. Maier for preparing the targets.

*Research work of K. A. Eberhard supported in part by U. S. Atomic Energy Commission.

†Present address: Nuclear Physics Laboratory, GL-10, University of Washington, Seattle, Washington 98195.

‡Permanent address: Department of Physics, Kansas State University, Manhattan, Kansas.

¹J. S. Blair, Phys. Rev. **95**, 1218 (1954).

²W. E. Frahn and R. H. Venter, Ann. Phys. (N. Y.) **24**, 243 (1963).

³Proceedings of the Symposium on Four Nucleon Correlations and Alpha Rotator Structure, Marburg, Germany, 1972, edited by R. Stock.

⁴Proceedings of the First Louvain-Cracow Seminar on

The Alpha-Nucleus Interaction, Cracow, Poland, 1973 (unpublished).

⁵R. H. Siemssen, J. V. Maher, A. Weidinger, and D. A. Bromley, Phys. Rev. Lett. **19**, 369 (1967); **20**, 175 (1968); J. V. Maher, M. W. Sachs, R. H. Siemssen, A. Weidinger, and D. A. Bromley, Phys. Rev. **188**, 1665 (1969); R. W. Shaw, R. Vandenbosch, and M. K. Mehta, Phys. Rev. Lett. **25**, 457 (1970).

⁶R. A. Chatwin, J. S. Eck, D. Robson, and A. Richter, Phys. Rev. C **1**, 795 (1970); D. Robson, in Proceedings of the Symposium on Heavy Ion Scattering, Argonne National Laboratory, 1971 (unpublished), p. 239, and literature cited therein.

- ⁷P. P. Urone, L. W. Put, B. W. Ridley, and G. D. Jones, Nucl. Phys. A167, 383 (1971); M. E. Cage, D. L. Clough, A. J. Cole, J. B. A. England, G. J. Pyle, P. M. Rolph, L. H. Watson, and D. H. Worledge, *ibid.* A183, 449 (1972); A. J. Buffa and M. K. Brussel, *ibid.* A195, 545 (1972).
- ⁸H. P. Morsch and R. Santo, Nucl. Phys. A179, 401 (1972); H. P. Morsch and H. Breuer, *ibid.* A208, 255 (1973).
- ⁹G. E. Mitchell, E. B. Carter, and R. H. Davis, Phys. Rev. 133, B1434 (1964).
- ¹⁰J. C. Corelli, E. Bleuler, and D. J. Tendam, Phys. Rev. 116, 1184 (1959).
- ¹¹J. F. Morgan and R. K. Hobbie, Phys. Rev. C 1, 155 (1970).
- ¹²R. A. Atnoesen, H. L. Wilson, M. B. Sampson, and D. W. Miller, Phys. Rev. 135, B660 (1964).
- ¹³T. Mikumo, J. Phys. Soc. Jpn. 16, 1066 (1961).
- ¹⁴D. E. Blatchley and R. D. Bent, Nucl. Phys. 61, 641 (1965).
- ¹⁵H. F. Lutz and S. F. Eccles, Nucl. Phys. 81, 423 (1966).
- ¹⁶J. W. Frickey, K. A. Eberhard, and R. H. Davis, Phys. Rev. C 4, 434 (1971).
- ¹⁷L. Seidlitz, E. Bleuler, and D. J. Tendam, Phys. Rev. 110, 682 (1958).
- ¹⁸B. T. Lucas, S. W. Cospers, and O. E. Johnson, Phys. Rev. 144, 972 (1966).
- ¹⁹W. J. Thompson, G. E. Crawford, and R. H. Davis, Nucl. Phys. A98, 228 (1967).
- ²⁰K. A. Eberhard and C. Mayer-Böricke, Nucl. Phys. A142, 113 (1970).
- ²¹K. A. Eberhard and D. Robson, Phys. Rev. C 3, 149 (1971).
- ²²H. J. Kim, Phys. Lett. 19, 296 (1965).
- ²³A. G. Drentje and R. D. A. Roeders, in Contributions to the Europhysics Study Conference on Intermediate Processes in Nuclear Reactions, Plitvice Lakes, Yugoslavia, 1972 (unpublished).
- ²⁴P. P. Singh, M. D. High, R. E. Malmin, and D. W. Devins, Nucl. Phys. A163, 289 (1971).
- ²⁵J. S. Vincent, E. T. Boschitz, and J. R. Priest, Phys. Lett. 25B, 81 (1967).
- ²⁶K. A. Eberhard and W. Trombik, Nucl. Phys. A193, 489 (1972).
- ²⁷A. G. Drentje and J. D. A. Roeders, Phys. Lett. 32B, 356 (1970).
- ²⁸O. H. Gailar, E. Bleuler, and D. J. Tendam, Phys. Rev. 112, 1989 (1958).
- ²⁹F. W. Bingham, Phys. Rev. 145, 901 (1966).
- ³⁰A. W. Obst and K. W. Kemper, Phys. Rev. C 6, 1705 (1972).
- ³¹K. Chyla, H. Niewodniczanski, J. Szymakowski, U. Tomza, and H. Wojciechowski, Institute of Nuclear Physics Cracow, Report No. 699/PL, 1970 (unpublished).
- ³²B. T. Lucas, S. W. Cospers, and O. E. Johnson, Phys. Rev. 135, B116 (1964).
- ³³H. Schmeing and R. Santo, Phys. Lett. 33B, 219 (1970).
- ³⁴H. L. Wilson and M. B. Sampson, Phys. Rev. 137, B305 (1965).
- ³⁵C. B. Fulmer, J. Benveniste, and A. C. Mitchell, Phys. Rev. 165, 1218 (1968).
- ³⁶P. T. Sewell, J. C. Hafele, C. C. Foster, N. M. O'Fallon, and C. B. Fulmer, Phys. Rev. C 7, 690 (1973).
- ³⁷M. Ivascu, G. Semenescu, D. Bucurescu, and M. Titirici, Nucl. Phys. A147, 107 (1970).
- ³⁸W. Trombik, K. A. Eberhard, G. Hinderer, H. H. Rossner, A. Weidinger, and J. S. Eck, Phys. Rev. C 9, 1813 (1974).
- ³⁹O. F. Lemos, Ph.D. thesis, Faculté des Sciences d'Orsay, 1972 (unpublished).
- ⁴⁰R. Bock, P. David, H. H. Duhm, H. Hefele, U. Lynen, and R. Stock, Nucl. Phys. A92, 539 (1967).
- ⁴¹A. E. Bisson, K. A. Eberhard, and R. H. Davis, Phys. Rev. C 1, 539 (1970).
- ⁴²K. A. Eberhard, Phys. Lett. 33B, 343 (1970).
- ⁴³W. Henning, R. Müller, K. E. Rehm, and H. Schaller, Beschleunigerlaboratorium der Universität und der Technischen Universität München, Annual Report 1970 (unpublished), p. 32.
- ⁴⁴J. G. Cramer, K. A. Eberhard, J. S. Eck, and W. Trombik, Phys. Rev. C 8, 625 (1973).
- ⁴⁵K. A. Eberhard, in Proceedings of the First Louvain-Cracow Seminar on the Alpha-Nucleus Interaction, Cracow, Poland, 1973 (see Ref. 4), p. 103.
- ⁴⁶R. Vandenbosch, M. P. Webb, and M. S. Zisman, Phys. Rev. Lett. 33, 842 (1974).
- ⁴⁷T. Tamura, Rev. Mod. Phys. 37, 679 (1965); Nucl. Phys. 73, 81 (1965); Oak Ridge National Laboratory Report No. 4152, 1967 (unpublished).
- ⁴⁸H. Rebel and G. W. Schweimer, Kernforschungszentrum Karlsruhe Report No. KFZ 1333, 1971 (unpublished).
- ⁴⁹G. Gaul, H. Lüdecke, R. Santo, H. Schmeing, and R. Stock, Nucl. Phys. A137, 177 (1969).
- ⁵⁰J. Schiele and K. A. Eberhard, Verhandl. DPG(VI) 8, 138 (1973); and unpublished.
- ⁵¹W. J. Thompson, J. S. Eck, K. A. Eberhard, J. Schiele, and W. Trombik, unpublished.
- ⁵²T. Ericson and T. Mayer-Kuckuk, Annu. Rev. Nucl. Sci. 16, 183 (1966).